Heterogeneous Reactions on Sulfuric Acid Films with Implications for Ozone Depletion

by

Rosemary Elizabeth Koch

B.S. Chemistry
Manhattan College, 1993

Submitted to the Department of Chemistry in Partial Fulfillment of the requirements for the degree of

Master of Science in Chemistry
at the
Massachusetts Institute of Technology

June 1996

Signature of Author.....
Department of Chemistry
May 24, 1996

Certified by.....
Mario Molina
Martin Professor of Atmospheric Chemistry
Thesis supervisor

Accepted by.....
Dietmar Seyferth
Chairman, Departmental Committe on Graduate Students

Heterogeneous Reactions on Sulfuric Acid Films with Implications for Ozone Depletion

by

Rosemary E. Koch

Submitted to the Department of Chemistry on May 24, 1996, in partial fulfillment of the requirements for the degree of Master of Science in Chemistry

Abstract

Vapor pressure measurements of HCl in ternary $H_2SO_4/H_2O/HCl$ and quaternary $H_2SO_4/H_2O/HNO_3/HCl$ solutions were measured. Henry's law constants were determined and were found to be in good agreement with published semiempirical models. Reaction probabilities for the reaction $HCl + ClONO_2$ were measured on thin films of sulfate solutions with compositions simulating those of stratospheric aerosols. It was observed that the reaction probability increases dramatically as the stratospheric aerosols become more dilute at low temperatures. The parameter that controls the reaction probability appears to be the HCl solubility. Uptake of HNO_3 has a small but measurable effect on γ. These results give evidence to the hypothesis that supercooled liquid sulfate aerosols promote chlorine activation in the stratosphere at low temperatures as efficiently as solid polar stratospheric cloud particles.

Thesis Supervisor: Mario J. Molina
Title: Martin Professor of Atmospheric Chemistry

Acknowledgments

I would like to thank Mario Molina and all the members of the Molina lab for their help and guidance throughout my time at MIT. In particular, I would like to thank Matt Elrod for working with me on the wetted wall flow technique, and teaching me most of what I know about flow tube techniques and Carl Percival for his help in getting this thesis into a (hopefully) readable form.

I would also like to thank my parents, for their unconditional love and support no matter what I do, and Vanessa and Mike for always being there for me.

Contents

List of Figures

List of Tables

Chapter 1
Introduction

Ozone is an important constituent in the stratosphere, although it's ambient concentration does not exceed 10 ppmv. Since it absorbs ultraviolet light in the 240-290 nm region which is damaging to living cells, it is essential to life as we know it. In addition, this absorption of radiation leads to heating of the atmosphere which affects the temperature structure of the atmosphere which in turn drives meteorological processes. (Wayne, 1991) Steady state decreases in ozone concentrations and the corresponding increase in UV light reaching the Earth's surface have global implications.

1.1 The Ozone Layer

The so-called "ozone layer" is centered at an altitude of 25-30 km In this region, ozone is in a state of dynamic equilibrium, being continually produced and destroyed. The

natural production and destruction mechanism was first proposed by Chapman (1930). Chapman explained the existence of the ozone layer by the following set of reactions:

$$O_2 + h\nu\ (\lambda = 130\text{-}175\ \text{nm}) \rightarrow O + O \qquad (1.1)$$

$$O + O_2 + M \rightarrow O_3 + M \qquad (1.2)$$

$$O_3 + h\nu\ (\lambda = 240\text{-}290\ \text{nm}) \rightarrow O + O_2 \qquad (1.3)$$

$$O + O_3 \rightarrow 2O_2 \qquad (1.4)$$

The Chapman mechanism helps explain the existence of the ozone layer. At high altitudes, little ozone is produced since the pressure is low and there are few O_2 molecules to be photolyzed to O atoms. In addition, reaction 1.2 is a three body reaction which is not efficient at low pressures. The ozone layer is therefore formed at altitudes where the number density of oxygen molecules is high enough so that reactions 1.1 and 1.2 are efficient, and there is enough UV light to effectively form O atoms to initiate the cycle.

Ozone is photochemically produced mostly in the tropics, at high altitudes and is then transported to the poles where it accumulates. The highest abundances of ozone are found at high latitudes (Wayne, 1991).

1.2 Ozone Depletion

The Chapman scheme predicts higher ozone levels than are observed in the atmosphere (Wayne, 1991). Bates and Nicolet (1950) suggested that catalytic atmospheric processes that remove O or O_3 could explain the discrepancy between

observed and predicted stratospheric O_3 levels. The simplest of these reactions have the general form

$$X + O_3 \rightarrow XO + O_2 \tag{1.5}$$

$$XO + O \rightarrow X + O_2 \tag{1.6}$$

$$\text{net: } O + O_3 \rightarrow 2O_2$$

where X is typically H, OH, NO, Cl. and Br, although other cycles may participate. In addition to the single species chemistry, cycles of each of the species interact with each other producing many other cycles.

The trace gases come from several sources, both natural and anthropogenic. OH is formed in the stratosphere by the reaction of excited oxygen atoms with naturally occurring water vapor and methane. The main source of stratospheric NO_x is N_2O which is produced at the earth's surface by bacteria in soil and water, and is somewhat increased by the use of fertilizers. Chlorine comes mainly from anthropogenic sources.

1.2.1 Chloroflorocarbons

In the 1930's, chloroflorocarbons (CFCs) were developed by the General Motors Research Laboratories as a non-toxic, non-flammable refrigerant. These compounds are remarkably unreactive and have been used for a variety of applications. The four main uses for CFCs are refrigerants, cleaning fluids, propellants, and blowing agents for making plastic foam (Pool, 1988).

Early in the 1970's, it was noted that CFCs were present in the troposphere (Lovelock, 1973). Subsequent research has indicated that CFCs have extremely long

lifetimes in the atmosphere (from 60 - 522 years) and can be transported to the stratosphere (Wayne, 1991). Once CFCs are transported to the stratosphere, they can be photolyzed to produce chlorine atoms:

$$CF_2Cl_2 + h\nu\,(170\text{-}260\text{ nm}) \rightarrow CF_2Cl + Cl \qquad (1.7)$$

It was recognized that since chlorine can participate in catalytic cycles which deplete ozone, this source of chlorine in the stratosphere has dramatic implications for the ozone layer (Molina and Rowland, 1974).

1.2.2 The Ozone Hole

In 1985, the discovery of the Antarctic ozone "hole" revealed that ozone was definitely being depleted in the stratosphere. These measurements showed that the total ozone column density over Antarctica decreased by as much as 50% during the polar spring (Farman, 1985).

1.2.2a Polar Meteorology

The dramatic loss of ozone in the Antarctic stratosphere is a result of unique polar meteorology. After the autumnal equinox, the polar region enters a period of darkness and solar ultraviolet heating ends. The stratosphere cools and a pressure gradient develops between the pole and mid-latitudes. This combined with the Earth's rotation creates westerly winds with speeds reaching in excess of 100 ms^{-1} which circle the pole creating a polar vortex. This effectively isolates the portion of the stratosphere where

ozone depletion is noted. During the dark polar winter temperatures can reach below -90°C (Schoeberl and Hartman, 1991).

1.2.2b Gas Phase Ozone Depletion Chemistry

Taking into account the cold temperatures in the polar vortex and the increase in anthropogenic Cl from CFCs, the following mechanism was proposed to help account for the formation of the ozone hole (Molina and Molina, 1987).

$$ClO + ClO + M \rightarrow (ClO)_2 + M \quad (1.8)$$

$$(ClO)_2 + h\nu \rightarrow Cl + ClOO \quad (1.9)$$

$$ClOO + M \rightarrow Cl + O_2 + M \quad (1.10)$$

$$2(Cl + O_3 \rightarrow ClO + O_2) \quad (1.11)$$

$$\text{net:} \quad 2O_3 + h\nu \rightarrow 3O_2$$

This process is only important at the poles, as low temperatures and high ClO concentrations are necessary for the formation of the $(ClO)_2$ dimer.

In addition, it has been suggested that chlorine and bromine are coupled together in ozone destruction (McElroy *et al.*, 1986):

$$ClO + BrO \rightarrow Cl + Br + O_2 \quad (1.12)$$

$$Cl + O_3 \rightarrow ClO + O_2 \quad (1.13)$$

$$Br + O_3 \rightarrow BrO + O_2 \quad (1.14)$$

$$\text{net: } 2O_3 \rightarrow 3O_2$$

These cycles can be terminated by the reaction of active chlorine with methane and NO_2 which results in the formation of HCl and $ClONO_2$ which are relatively inactive with respect to ozone destruction:

$$Cl + CH_4 \rightarrow HCl + CH_3 \quad (1.15)$$

$$Cl + NO_2 + M \rightarrow ClONO_2 \quad (1.16)$$

Much of the free chlorine in the stratosphere is constrained in these so-called "reservoir" species HCl and $ClONO_2$ which are practically unreactive in the gas phase; the gas phase reaction HCl + $ClONO_2$ has an upper limit of 10^{-19} molecule^{-1} cm^{3}s^{-1} (Molina *et al.*, 1985).

1.2.2c Polar Stratospheric Clouds

Traditional gas phase chemistry alone cannot account for the magnitude of ozone destruction observed in the polar springtime (Wayne, 1991). However, another feature of the polar vortex helps explain the discrepancy between model predictions and actual ozone depletion. It has been known for a long time that visible, mother-of-pearl or nacreous clouds may occur at stratospheric altitudes in polar regions. These clouds are created by a sudden drop in temperature below 190 K and the condensation of water vapor (Stanford and Davis, 1974). More recently, it has been established that polar stratospheric clouds exist at warmer temperatures, and thus must be composed of something other than pure water. Observations by the Stratospheric Aerosol Measuring Instrument (SAM II) showed PSCs existing at temperatures as high as 196 K (McCormick *et al.*, 1982). It was originally assumed that PSCs are solid particles consisting of either nitric acid

trihydrate (NAT) or water ice (Molina, 1994), but recent research gives cause to question the phase of PSCs.

Although it has been assumed that heterogeneous processing in the Antarctic takes place on solid media, it has been suggested that liquid aerosols may also be important (Molina *et al.*, 1993). Analyses of *in situ* observations of PSC particles is lending evidence to the hypotheses that liquid sulfate aerosols may play an important role in polar ozone depletion. Toon and Tolbert analyzed infrared spectra of type I PSCs and found that they were not composed of NAT but could perhaps be liquid ternary solutions. In addition, field measurements have shown that there is a sharp jump in aerosol volume at a temperature which is near the NAT frost point (Kawa *et al.*, 1992). This has often been interpreted as evidence for solid formation, but new studies indicate that liquid aerosol particles absorb large amounts of H_2O and HNO_3 vapors as the temperature approaches a threshold value which happens to coincide with the NAT frost point. Thus it seems that the field measurements are more consistent with the existence of supercooled liquid sulfate aerosols with high HNO_3 than with the existence of solid particles liquid aerosol particles (Carslaw *et al.*, 1994; Drla *et al.*, 1994).

1.2.2d Heterogeneous Reactions

PSCs and sulfate aerosols can serve as reaction surfaces and facilitate the conversion of normally unreactive reservoir species into photochemically active chlorine species Cl and ClO. (Solomon *et al.*, 1986 and McElroy *et al.*, 1986). In addition, PSCs sequester NO_x in the condensed phase which decreases the rate of reaction 1.16 and thus

increase the amount of active chlorine that is available to take place in ozone depletion reactions.

The heterogeneous reactions of importance are

$$ClONO_2 + HCl \rightarrow Cl_2 + HNO_3 \quad (1.17)$$

$$ClONO_2 + H_2O \rightarrow HOCl + HNO_3 \quad (1.18)$$

$$HOCl + HCl \rightarrow Cl_2 + H_2O \quad (1.19)$$

$$N_2O_5 + H_2O \rightarrow 2HNO_3 \quad (1.20)$$

$$N_2O_5 + HCl \rightarrow ClONO_2 + HNO_3 \quad (1.21)$$

It was first shown that reactions 1.17 and 1.19 (Molina *et al.*, 1987) and 1.20 and 1.21 (Tolbert *et al.*, 1988) are indeed effective on ice surfaces, thus demonstrating the importance of heterogeneous reactions to ozone depletion. Later laboratory work has demonstrated the effectiveness of NAT as a medium for heterogeneous reactions (Abbatt and Molina, 1992a; Hanson and Ravishankara, 1991).

Laboratory measurements have also demonstrated the effectiveness of liquid aerosols as a heterogeneous medium. The rates of heterogeneous reactions are a strong function of chemical composition and phase of the aerosols. The hydrolysis of N_2O_5, (reaction 1.20) occurs rapidly on all liquid sulfate aerosols, with little dependence on temperature, composition or particle size. (Mozurkewich and Calvert, 1988; Van Doren *et al.*, 1991; Hanson and Ravishankara, 1991) Reaction 1.17 and 1.18, on the contrary are strong functions of compositions, with higher rates for more dilute aerosols. (Tolbert *et al.*, 1988; Hanson and Ravishankara, 1993; 1994; Zhang *et al.*, 1994).

The evidence that supercooled liquid aerosols may exist at the poles even at very low temperatures, combined with the experimental evidence that cold sulfate aerosols can efficiently activate chlorine indicates that sulfate aerosols may be an important factor in ozone depletion at the poles.

1.3 Liquid Sulfate Aerosols at Middle Latitudes

Sulfate aerosols are ubiquitous in the stratosphere, existing at altitudes between 25 and 30 km. They are composed mainly of aqueous sulfuric acid in the 60-80 weight % range, with the H_2SO_4 concentration decreasing as the temperature drops. The composition of aerosols is determined by temperature and water vapor mixing ratios, as aerosols remain in equilibrium with environmental water vapor by absorbing or evaporating H_2O as a function of temperature (Rosen, 1971, and Steele, 1983).

At temperatures below 210 K, sulfate aerosols absorb H_20, HNO_3 and small amounts of HCl to form supercooled ternary $H_2SO_4/H_2O/HNO_3$ solutions and quaternary $H_2SO_4/H_2O/HNO_3/HCl$ solutions (Molina *et al.*, 1993; Zhang *et al.*, 1993; Tabazadeh *et al.*, 1993).

There is increasing evidence that heterogeneous chemistry may occur on sulfate aerosols that may contribute to ozone depletion at mid-latitudes (Hofmann and Solomon, 1989; Arnold *et al.*, 1990; Rodriguez *et al.*, 1991). Ozone measurements from 1979 to 1994 show that trends in middle latitudes are significantly negative in all seasons. Northern hemisphere measurements show an ozone depletion rate of about 6% per decade

in the winter/spring, and 3% per decade in the summer/autumn. (WMO, 1994) This mid-latitude depletion could be in part caused by reactions on sulfate aerosols.

It is important to understand heterogeneous processes on sulfate particles because they may have greater implications for ozone depletion under perturbed stratospheric conditions (Golden *et al.*, 1994). Major volcanic eruptions can greatly perturb the normal background loading of aerosols. It has been proposed that increased stratospheric aerosol loadings may significantly decrease global ozone concentrations. As evidence, recent AASE II observations reveal significant decreases in both $ClONO_2$ and HCl concentrations after the eruption of Mt. Pinatubo, although a meteorological analysis did not indicate the formation of PSCs. (Toon *et al.*, 1993) This adds validity to the hypothesis that heterogeneous processing can occur at mid-latitudes under conditions of extreme sulfate loading, although at mid-latitudes, the sulfate aerosols speed up only reaction 1.20.

1.4 Aims of this Work

Since previous work has suggested that sulfate aerosols may play a role in explaining ozone depletion both in the Antarctic and in mid latitudes, it is necessary to study these aerosols in more depth. In order to truly quantify the extent to which heterogeneous reactions on sulfate aerosols play a role in ozone depletion, it is necessary to study these reactions in a laboratory setting and parameterize the reaction rates for use in models. First, since the reaction rate is partially determined by aerosol composition, it is necessary to fully characterize sulfuric acid solutions as a function of temperature.

Secondly, it is necessary to determine reaction rates, solubilities and diffusion rates as a function of temperature.

This thesis explores in greater depth reactions on sulfate aerosols. Chapter 2 describes the wetted wall-flow tube technique used in the experimental investigations discussed in subsequent chapters. Chapter 3 describes experimental determinations of Henry's Law constants for HCl in ternary and quaternary sulfate aerosols. Chapter 4 gives further details about reaction rates on sulfate aerosols, including temperature and compositional dependencies. Chapter 5 discusses the implications of these findings for the stratosphere and mentions further research that should be performed to get a more complete picture of the role of stratospheric sulfate aerosols in ozone depletion.

Chapter 2
Experimental Design

Reaction probabilities for the $ClONO_2$ + HCl reaction and HCl vapor pressures in sulfuric acid solutions were measured using a vertical wetted-wall flow tube coupled to a differentially pumped molecular beam sampling quadrupole mass spectrometer with an electron impact ionization scheme.

2.1 Experimental Approach

Laboratory measurements on micron sized aerosol particles simulating those in the stratosphere are extremely difficult, so laboratory studies are typically done on thin films (≈1 mm thick). Although these experiments do not simulate all stratospheric conditions, they provide useful information which can be applied to the stratosphere. They can give

information as to which of the aerosol constituents effect the rate constant most dramatically. For example, experimental measurements indicate that the reaction probability (γ) for reaction 1.17 is controlled by the concentration of HCl, as will be discussed in the Chapter 4.

Laboratory measurements of γ always give an upper limit for γ's on aerosol. With careful analysis, and some correction factors, laboratory γ's can be applied directly to aerosol particles. Hanson *et al.* (1994) give an in depth discussion of the circumstances when laboratory measurements can be directly applied to the stratosphere and provide a formalism for correcting laboratory measurements performed on liquid films. In order to use their framework, several fundamental parameters must be measured; rate constants, or reaction probabilities, and solubilities.

The vertical flow tube configuration allowed the surface of the liquid to be continually replenished, thus eliminating possible reactive depletion of constituents at the surface. All solutions were made up in the bulk to similate stratospheric compositions using the semi-empirical thermodynamic method of Carslaw *et al.* (1995) which yields vapor pressures as a function of liquid composition. Thus, it was possible to effectively decouple laboratory temperature from atmospheric temperature by preparing a fixed composition and changing the laboratory temperature. This was important because supercooled acid solutions have a tendency to freeze at very low temperatures, so it was necessary to measure reaction probabilities at temperatures above the atmospheric equilibrium temperatures.

2.2 The Flow Tube

The experimental apparatus is shown in figure 2.1. It consists of a vertically aligned flow tube with a cooling jacket. Attached to the top of the flow tube is a "liquid delivery system"--an annular cup with inlets for He carrier gas and a injector for $ClONO_2$. The solution of interest is pre-cooled and allowed to flow into the cup which overflows to create a falling cylindrical film of acid which coats the walls of the flow tube.

This wetted wall technique has been widely used in the field of chemical engineering and Danckwerts has described the fluid dynamics of such flow. A similar technique was used by Utter *et al.* (1992) to measure ozone uptake on aqueous surfaces.

The thickness of the liquid film is given by

$$\delta = \left(\frac{3\mu V}{\pi g d \rho} \right)^{\frac{1}{3}} \tag{2.1}$$

μ = viscosity of the liquid ($g \cdot cm^{-1} s^{-1}$)

V = volumetric flow rate ($cm^3 s^{-1}$)

g = acceleration do to gravity (980 $cm \cdot s^{-2}$)

d = flow tube diameter (2.4 cm)

ρ = density of the fluid ($g \cdot cm^{-3}$)

For the conditions of this experiment, $\mu \approx .5$ - 1.5, $V \approx 1$, and $\rho \approx 1.5$ so the liquid film was approximately 0.07 - 1 mm.

The velocity of the fluid at the surface is given by

$$v = \frac{3}{2}\left(\frac{V}{\pi d}\right)^{\frac{2}{3}}\left(\frac{gp}{3\mu}\right)^{\frac{1}{3}} \qquad (2.2)$$

The surface velocity was calculated to be 2.2-3.1 $cm \cdot s^{-1}$ for a flow rate of 1 $cm^3 \cdot s^{-1}$.

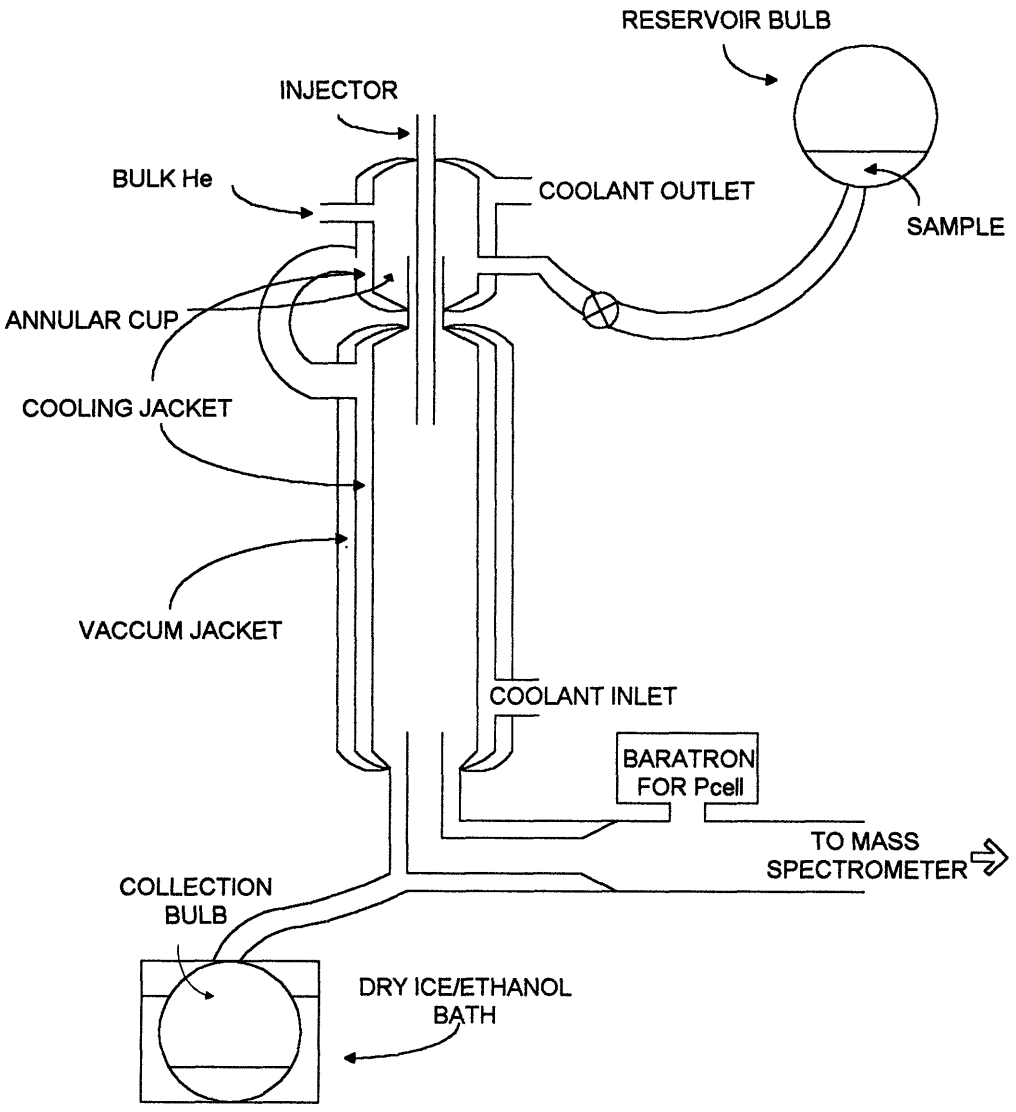

Figure 2.1 Apparatus for wetted-wall flow tube technique

During the course of an experiment, it was not possible to flow the acid and maintain a stable, cold temperature. Thus, when an experimental measurement was taken the walls were coated and the flow was turned off. It was assumed that thermal equilibrium was reached when the HCl signal was observed to stabilize (on the order of a few minutes). The flow tube wall was rinsed with fresh solution for each measurement in order to minimize the possible effects of dehydration; Hanson and Ravishankara (1991) showed that there is insignificant dehydration under similar reaction conditions. The carrier gas was sampled at the end of the flow tube and directed to the detection system. Used acid was collected at temperatures below that of the flow tube in order to prevent the backstreaming of vapors.

Most measurements were made with flow tube pressures of about 1 Torr and carrier gas flow velocities of about 1000 $cm \cdot s^{-1}$. The flow at this pressure is characterized in the laminar flow regime. The flow regime is described by the Reynolds number

$$Re = \frac{2r\rho v}{\mu} \tag{2.3}$$

r = flow tube radius

ρ = gas density

v = linear velocity

μ= gas viscosity

A Reynolds number >3000 indicates turbulent flow; lower than 2000 indicates laminar flow. Since we are working at low pressures, our conditions are well within the

region of laminar flow (Re ≈ 30). In the laminar flow regime, the rate of gas phase diffusion is very rapid, and as a result there is a high collision frequency with the acid-coated walls. In the laminar flow region, at low pressures, the "plug flow" approximation is used, that is it is assumed that all reactant molecules travel at the same axial velocity, because they effectively sample all radial positions. Using this approximation, reaction time can be calculated from the distance the injector is moved:

$\Delta t = \Delta p/\mu$ where t is time (s) and p is the injector position (cm).

2.3 The Mass Spectrometer

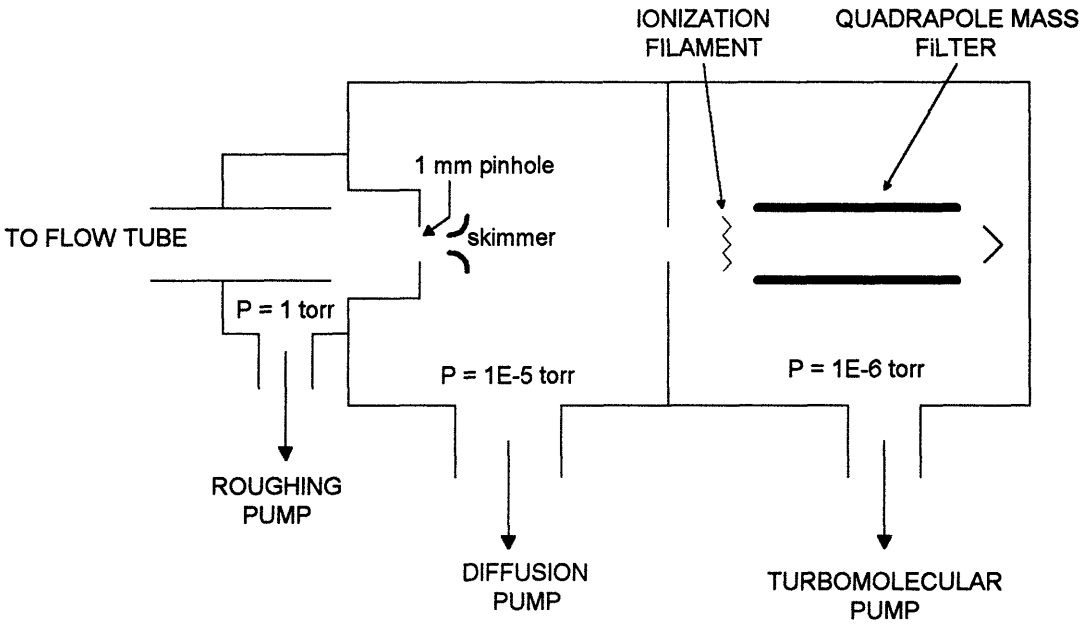

Figure 2.2 Schematic of Differentially Pumped Mass Spectrometer

A schematic of the mass spectrometer is shown in figure 2.2. The flow tube is separated from the first chamber by a 1.0 mm pin hole which can be closed with an O-ring

seal. The majority of the gas from the flow tube is removed by a roughing pump before the first chamber. The gas that does enter the mass spectrometer first passes through the initial pin hole into the first chamber which is pumped by a diffusion pump and is operated at approximately 10^{-5} Torr . This gas is collimated by a skimmer cone with a 1.0 mm hole. The resulting molecular beam goes into the second chamber which is pumped by a turbomolecular pump to a pressure of 10^{-6} Torr. In this chamber, the beam is chopped. This second chamber contains the ionization regain and the quadrapole. The output is amplified and detected with a lock-in amplifier.

2.4 Sample Preparation

Ternary and quaternary solutions of $H_2SO_4/HCl/H_2O$ and $H_2SO_4/HNO_3/HCl/H_2O$ were prepared in bulk solutions by diluting 96% H_2SO_4, 70% HNO_3 and 37% HCl with deionized water. The solutions were spot checked for composition with density and standard acid-base titration measurements and agreed with the expected compositions.

Chapter 3

Aerosol Composition--HCl Vapor Pressure Measurements

This chapter describes experimental results of the determination of Henry's Law constants for HCl in ternary $H_2SO_4/H_2O/HCl$ solutions, as well as in nitric acid containing quaternary $H_2SO_4/H_2O/HNO_3/HCl$ solutions.

3.1 Introduction

Since it has been suggested that the reactions on sulfate aerosols are important to the global ozone balance, it is important to characterize these reactions, and quantify fundamental parameters in order that heterogeneous reactions can be effectively included in models of the atmosphere. Since, these reactions occur on liquid aerosols, it is important to be able to predict aerosol composition as a function of temperature in order to determine the effect aerosol composition has on reaction kinetics. The composition of

sulfate aerosols is extremely dependent on temperature. As an aerosol that is composed predominantly of sulfuric acid is cooled, the solubility of water and HNO_3 will increase, thus decreasing the relative sulfate concentration. HCl concentration also increases with decreasing temperature as it is more soluble in dilute sulfuric acid. This is why it is crucial to characterize aerosol composition as a function of temperature.

Van Doren *et al.* (1991), Reihs *et al.* (1990) and Zhang *et al.* (1993) have measured uptake of HNO_3 by aqueous sulfuric acid droplets using Knudsen flow cell techniques. HCl uptake has been examined by several groups over a wide range of temperatures and acid compositions. (Hanson and Ravishankara, 1993; Watson *et al.*, 1990 and Williams and Golden, 1993) It has been shown that there is little HNO_3 or HCl uptake below 210K but below that, solubility increases rapidly with decreasing temperature. Several models have been constructed to predict aerosol composition as a function of temperature (Carslaw *et al.*, 1995; Tabazadeh *et al.*, 1994).

There is a discrepancy in the literature about the correct Henry's law coefficient for HCl in sulfuric acid solutions. Measurements of Hanson and Ravishankara (1993) differ greatly from those of Zhang *et al.* (1993) In addition, few studies have been done the composition of the quaternary solutions. This chapter will discuss measurements that address both these issues.

3.2 Henry's Law Constants

Henry's law constants were calculated from measurements of HCl vapor pressure. The wetted wall technique is well suited for measuring vapor pressures because the

surface can be constantly refreshed, eliminating errors due to depletion of the surface. In addition, vapor pressures can be measured directly, eliminating dilution errors.

Henry's Law relates gas and liquid-phase concentrations for an ideal solution:

$$[HCl(aq)] = P_{HCl}H \tag{3.1}$$

H = Henry's law constant ($M \cdot atm^{-1}$)

[HCl(aq)] = HCl concentration in the liquid

P_{HCl} = Vapor pressure of HCl in the gas phase

Actual HCl vapor pressures depend upon both solubility and extent of dissociation.

$$HCl(g) \rightarrow HCl(aq) \tag{3.2}$$

$$HCl(aq) \rightarrow H^+ + Cl^- \tag{3.3}$$

$$[HCl]_{tot} = [HCl(aq)] + [Cl\text{-}] \tag{3.4}$$

An effective Henry's law constant (H*) is defined as

$$H^* = \frac{[HCl]_{tot}}{P_{HCl}} \tag{3.5}$$

Taking into account reaction 3.3 and 3.4, the effective Henry's law constant can be expressed in terms of the Henry's law constant for an ideal solution.

$$H^* = H\left(1 + \frac{K}{[H^+]}\right) \tag{3.6}$$

where K is the acid dissociation constant.

3.3 Vapor Pressure Measurements.

Measurements of HCl vapor pressure were made by coating the walls of the flow tube with the solution of interest, and waiting a few minutes for the temperature to

stabilize. The saturation of the carrier gas with HCl vapor was checked by directing the helium flow through the movable injector; the observed HCl signal did not change with injector position, thus confirming the equilibrium condition. The mass spectrometer was calibrated using known HCl vapor pressures, so the mass spectrometer signal corresponds directly to P_{HCl}. The detection limit for HCl (monitored at mass 36) using these methods was approximately 10^{-7} Torr.

3.4 Calibration

In order to determine absolute values for the HCl vapor pressures, the mass spectrometer was calibrated using extrapolated HCl/H_2O vapor pressure data of 9 Molal HCl from Fritz and Fuget (1956). A small flow of He (1-50 sccm) was directed through a bubbler containing 9 Molal HCl. This He/HCl flow was subsequently diluted by the main carrier gas (≈500sccm). This experimental setup is shown in figure 3.1. By successively diluting the He/HCl flow and adjusting the temperature from 50° c to -30° c, it was possible to determine absolute measurements for known HCl vapor pressures using the following formula.

$$P_{HCl} = \frac{f_1}{f_1 + f_2} \frac{P_{vap}}{P_{sat}} P_{tube} \tag{3.7}$$

where

P_{vap} = vapor pressure of 9 Molal HCl solution (Torr)
$= T^{3.498} e^{\frac{-5750}{T}}$
P_{sat} = pressure of bubbler (Torr)
P_{tube} = pressure in flow tube (Torr)
f_1 = flow of He through bubbler
f_2 = carrier gas flow

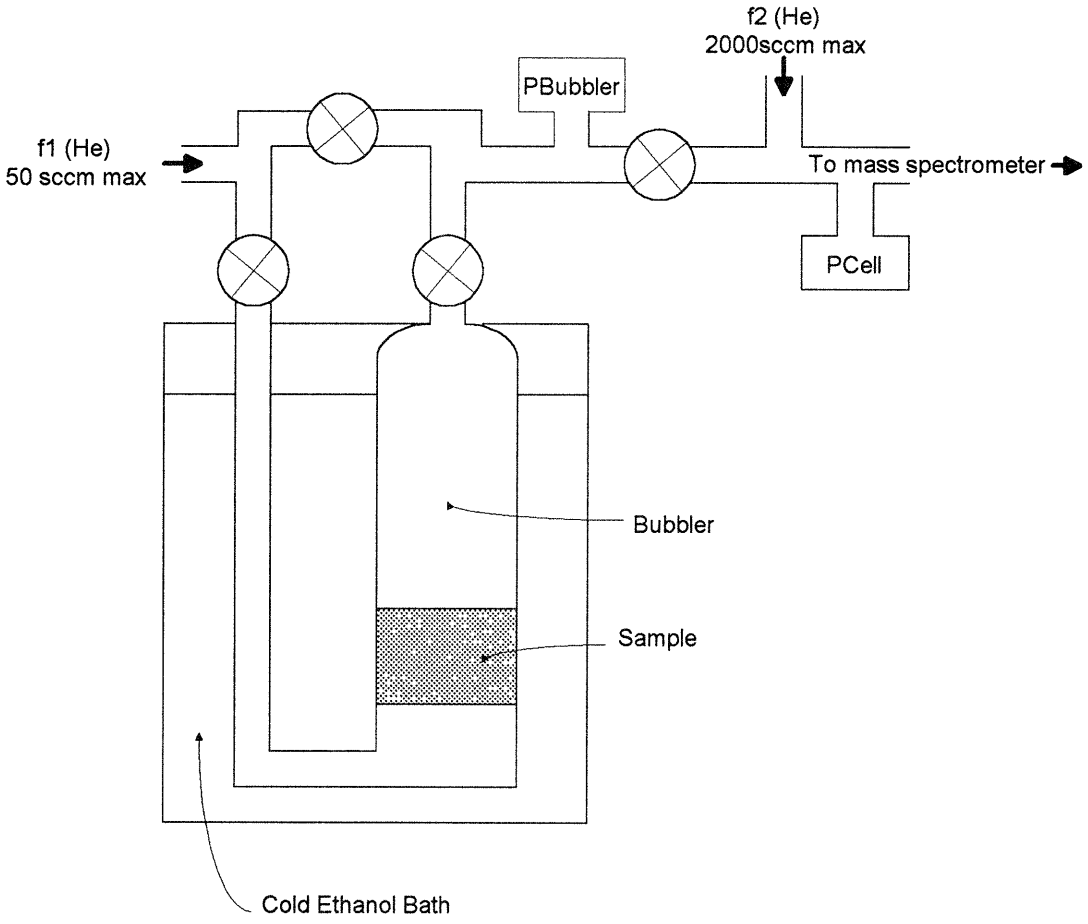

Figure 3.1 Calibration System

A sample calibration curve is shown in figure 3.2. In order to ensure that the mass spectrometer signal was stable, the calibration was performed both before and after each set of vapor pressure measurements. No noticeable drift in the mass spectrometer system was noted on the time scale of the measurements.

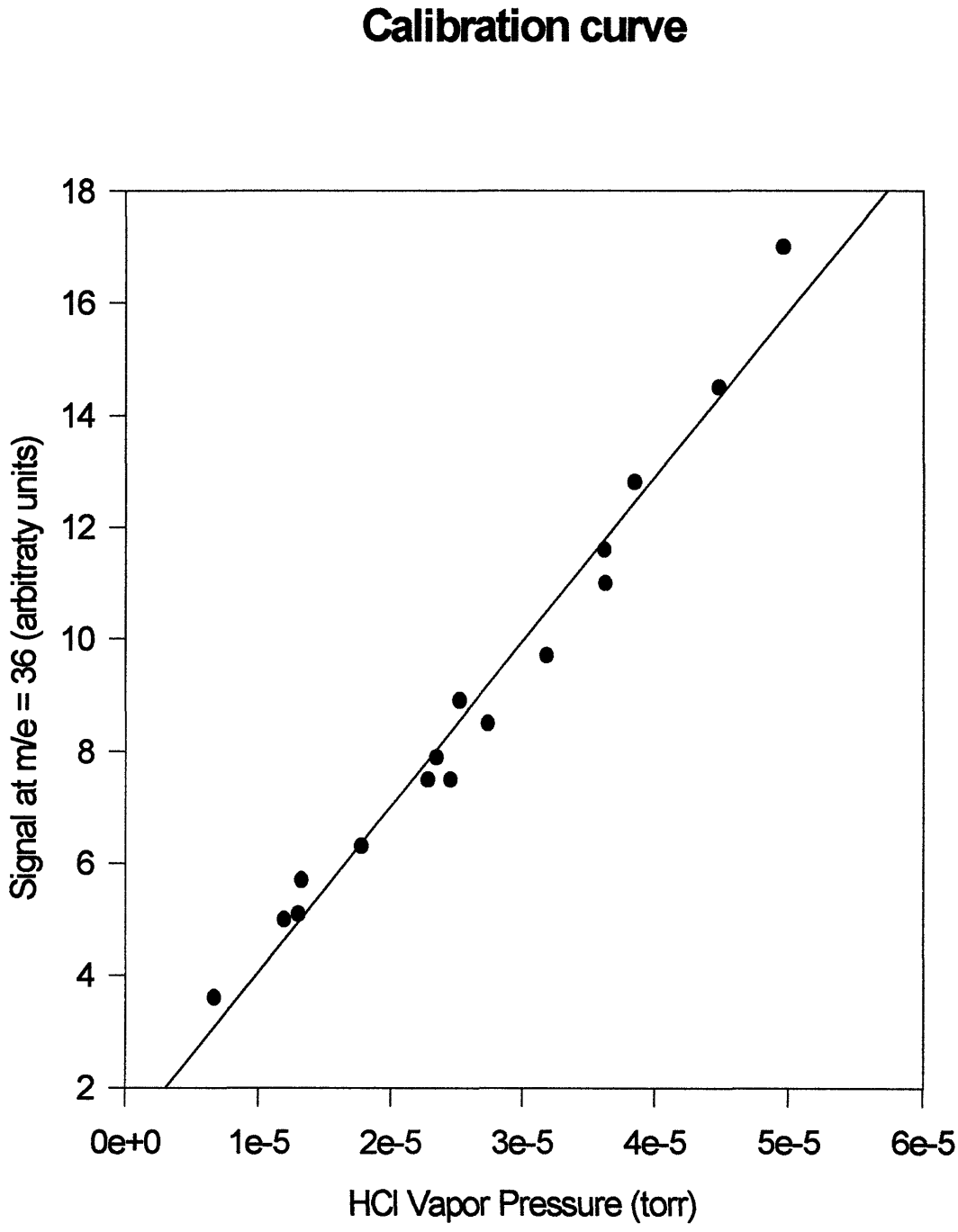

Figure 3.2 Calibration Curve for 9 Molal HCl

3.5 Results and Discussion

HCl vapor pressures were determined for 4 solutions: two ternary solutions (50% and 43% H_2SO_4) and two quaternary solutions 48% H_2SO_4; 3.5% HNO_3 and 36% H_2SO_4 and 12.5% HNO_3. This data is summarized in table 3.1.

Composition	T(K)	H*(M atm^{-1})
50 % H_2SO_4	225	4.0×10^5
9.2 x10^{-3} M HCl	222	5.2×10^5
	219	7.2×10^5
	216	9.8×10^5
	214	1.2×10^6
	211	1.8×10^6
	208	2.3×10^6
43 % H_2SO_4	226	2.5×10^6
3.0 x 10^{-2} M HCl	222	4.1×10^6
	218	6.8×10^6
	214	9.2×10^6
	208	1.8×10^7
48 % H_2SO_4	233	8.8×10^4
3.5 % HNO_3	231	1.1×10^5
3.9 x 10^{-3} M HCl	226	1.7×10^5
	222	2.7×10^5
	216	5.4×10^5
36.2 % H_2SO_4	228	5.5×10^5
12.5% HNO_3	223	1.2×10^6
6.2 x 10^{-3} M HCl	218	1.7×10^6
	213	2.8×10^6
	208	4.7×10^6

Table 3.1 Measured Henry's Law Solubility Constants

3.5.1 Ternary Solutions

The solubility of HCl was investigated in ternary solutions. One solution was chosen to directly compare with conflicting literature results (50 % H_2SO_4) This solution was examined for two different HCl concentrations: 9.2×10^{-3} M and 2.2×10^{-2} M. The Henry's law coefficients as a function of temperature are plotted in figure 3.3. The results are in good agreement with the data from Hanson and Ravishankara, as well as with the Carslaw *et al.* model, which implies that this model is useful to predict compositions of stratospheric aerosols. Our data varies considerable from Zhang *et al.*, but forms a consensus with the other literature values.

In order to test the Carslaw *et al.* model, for solutions directly applicable to the atmosphere, a solution of 43% H_2SO_4 was chosen. This composition corresponds to a stratospheric equilibrium temperature of 190K at 50 mbar, assuming 5 ppmv H_2O. The results are plotted in figure 3.4. The experimental results show good agreement with the Carslaw *et al.* model.

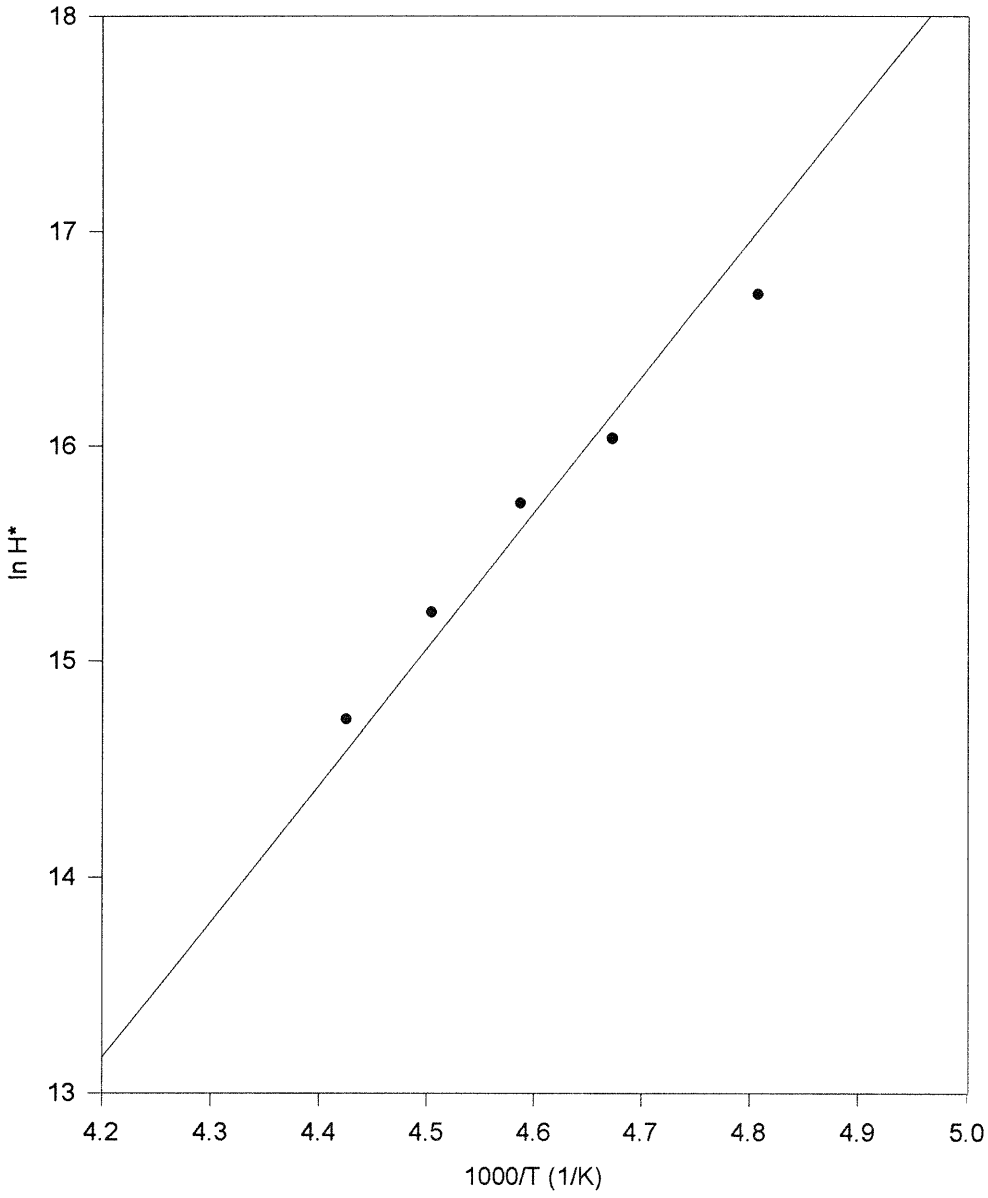

Figure 3.3 HCl Henry's Law constants as a function of temperature for 43% H_2SO_4. Circles represent data from this work. The solid line is estimated predictions from Carslaw *et al.* (1995).

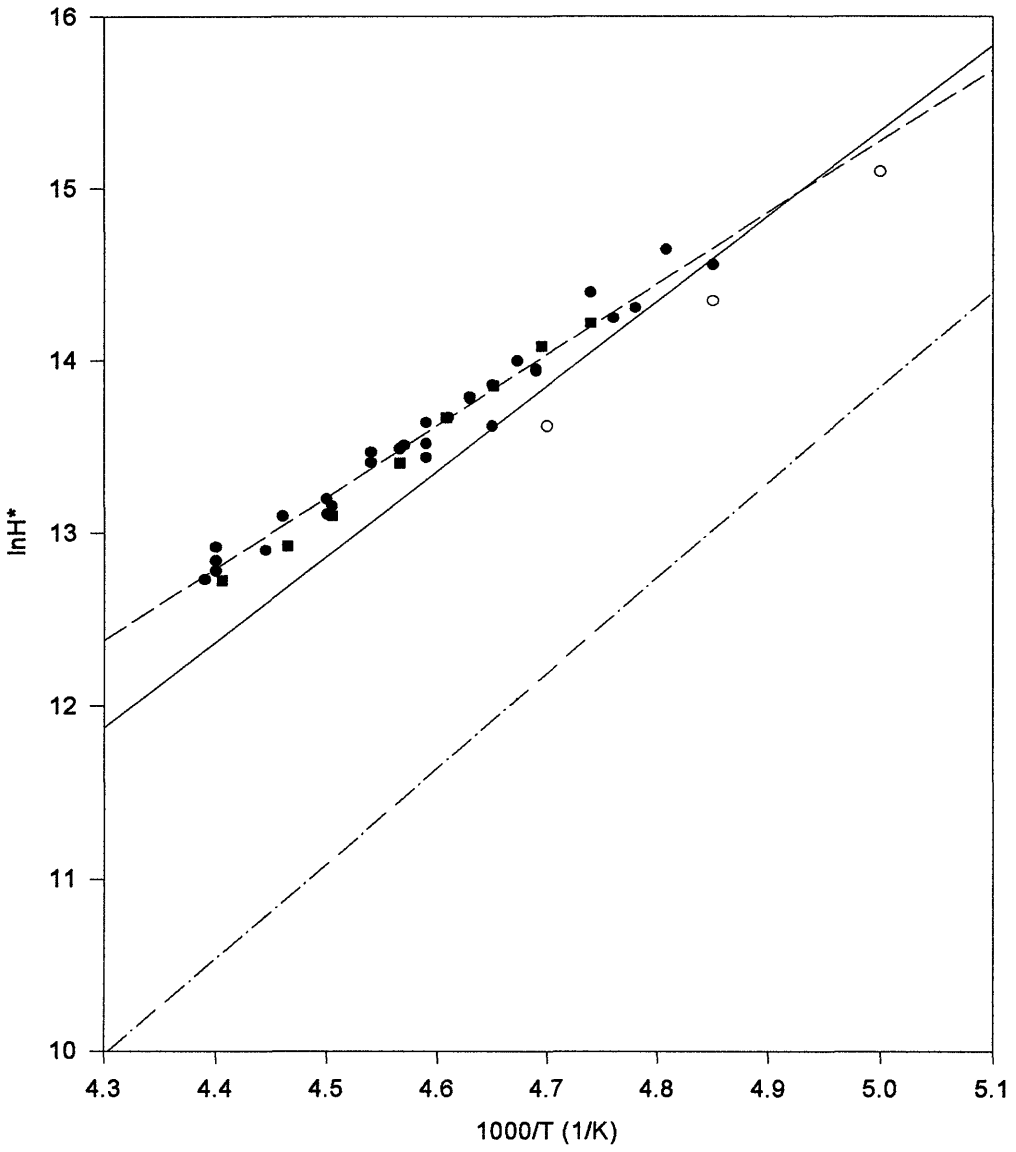

Figure 3.4 Henry's Law constants as a function of temperature for 50% H_2SO_4 solution. The solid circles represent solution with [HCl] = 9.2 x 10^{-3}, the solid squares [HCl] = 2.2 x10^{-2}. The dashed line is a fit of data from this work. Data from Hanson and Ravishankara (1993) is show by open circles. Carslaw *et al.* model predictions are shown as a solid line and the Zhang *et al.* (1993) parameterization is shown by the dot-dash line.

3.5.2 Quaternary Solutions

In order to spot check the HCl vapor pressures predicted by the Carslaw *et al.* model for $H_2SO_4/HNO_3/H_20/HCl$ quaternary solutions, two representative solutions were chosen. The compositions of these corresponds to atmospheric equilibrium temperatures of 198 K and 196 K at 100 mbar with 10 ppbv HNO_3 and 2 ppbv HCl. This data is summarized in Table 3.1. Figure 3.5 plots the measured lnH* for these solutions as a function of temperature, along with the predictions from the model. Our results are in good agreement with the model predictions.

Although our measurements were not intended to be an extensive test of the model's accuracy, they do imply that the model accurately predicts HCl solubility for the quaternary solutions, as well as the ternary solutions.

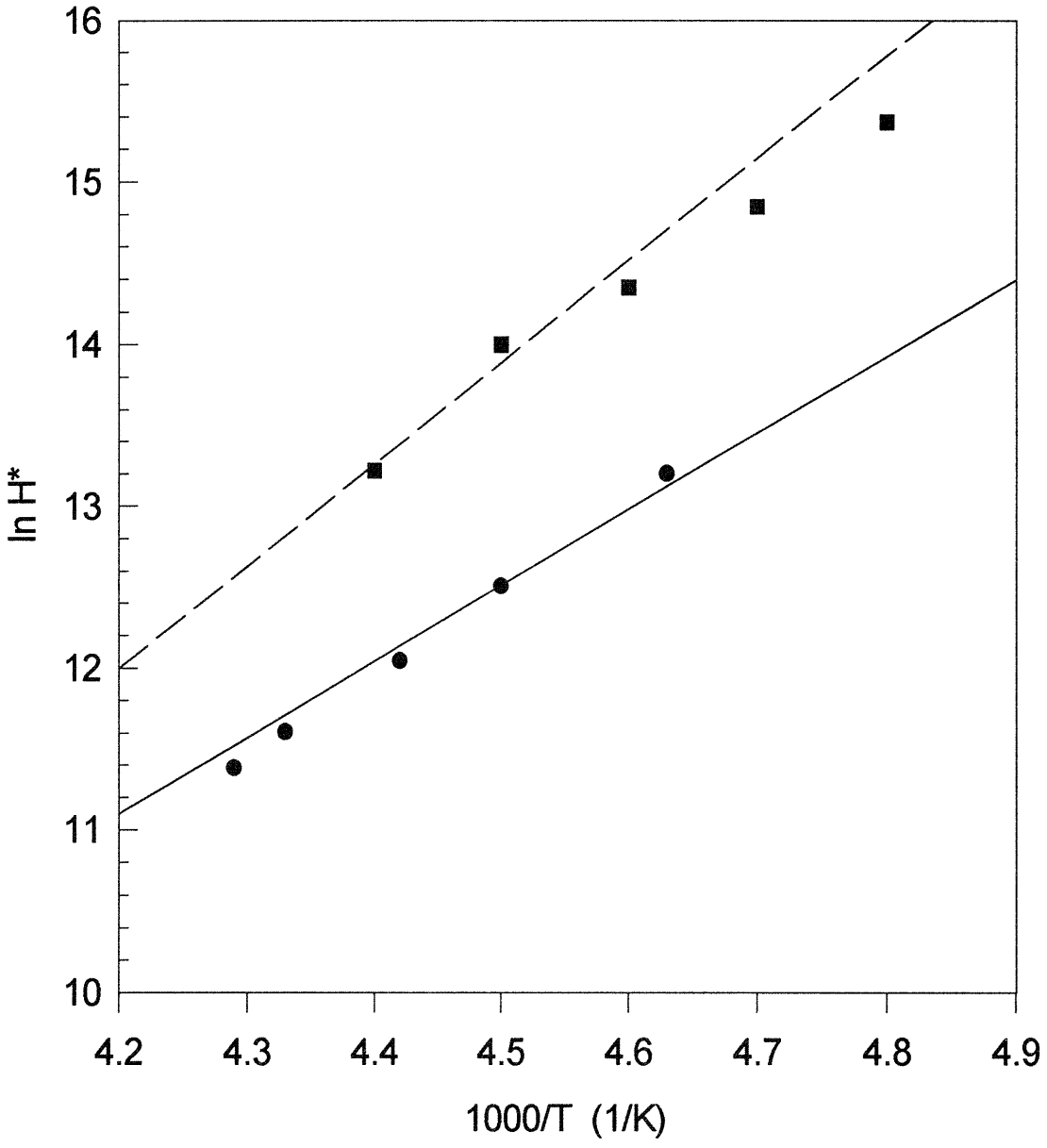

Figure 3.5 Henry's Law constants as a function of temperature for quaternary solutions. Squares and circles are data from this work. Lines are from the Carslaw *et al.* model. Squares and the dotted line are for the 36.2% H_2SO_4 - 12.5% HNO_3 solution. Circles and the solid line are for the 48% H_2SO_4 - 3.5% HNO_3 solution.

Chapter 4
Reaction Probabilities

The reaction probability, γ, is defined as the probability that a reaction will occur between two molecules when one of the particles collides with a surface that is covered to some extent with the other molecule.

This chapter focuses on the experimental determination of γ for reaction 1.17, $ClONO_2 + HCl \rightarrow Cl_2 + HNO_3$. Studies of this reaction have been done on a range of sulfuric acid solutions corresponding to stratospheric conditions, in order to understand the effect of stratospheric temperature and aerosol composition. In particular, the effect of HNO_3 incorporation into sulfate aerosols was examined.

4.1 Experimental Details

The focus of these experiments was to explore the threshold stratospheric temperature and corresponding concentrations at which reaction 1.17 becomes highly efficient in activating chlorine.

Acid solutions were chosen to correspond to typical stratospheric aerosols as predicted by Carslaw *et al.* (1995). These compositions were chosen by using the model to search for mixtures whose vapor pressures correspond to within 10% to atmospheric equilibrium temperatures assuming 5 ppmv H_2O and 2 ppbv HCl at 100 mbar (16 km altitude). Solutions were made to represent temperatures between 194 and 201K, both with and without HNO_3. The solutions without nitric acid varied from 43-55% H_2SO_4. The corresponding HCl weight per cents ranged from 8×10^{-4} to 3×10^{-6} . For the solutions containing nitric acid, the weight fraction H_2SO_4 varied from 20 to 50% and the nitric acid from 2-28%.

$ClONO_2$ partial pressures of about 1×10^{-6} Torr were used for the kinetics measurements and the possible reactive depletion of HCl was investigated for each solution. Because the electron impact ionization scheme results in the production of NO_2^+ for both $ClONO_2$ and HNO_3, it was necessary to detect the reaction product, Cl_2^+, for the quaternary solutions (since the ambient HNO_3 vapor pressures were high enough to interfere with the $ClONO_2$ signals). The measured first order rate constant k_m was determined by flowing $ClONO_2$ through a moveable injector which is incrementally moved back. k_m can be determined from a plot of signal (S) versus injector position (p).

$$k_m = \frac{d(\log S)}{dp} v \tag{4.1}$$

v = flow velocity

The reaction probability is given as

$$\gamma = \frac{2rk_m}{c} \tag{4.2}$$

r = flow tube radius

c = thermal velocity of the molecules which is defined as

$$c = \left(\frac{8RT}{\pi M}\right)^{\frac{1}{2}} \tag{4.3}$$

When γ is large, strong radial concentration gradients may develop in the flow tube. These effects can be accounted for in the analysis and determination of γ by standard cylindrical flow tube techniques (Brown 1978, Howard 1979).

4.2 Results

A typical kinetics plot of signal versus injector distance is shown in figure 4.1. Since this solution (198K) contains no HNO_3, both the loss of the reactant $ClONO_2$ and the production of the product Cl_2 could be observed. The rise of Cl_2^+ and the decay of NO_2^+ are plotted. Comparable values of k_m are obtained, this confirming the validity of

using the m/e=70 peak for kinetics measurements when the NO_2^+ peak can't be used, as a result of a contribution from HNO_3.

The reaction probability increased rapidly over the range of solutions studied, from 0.01 for the 201K (no nitric) solution to 0.3 for the 194K solution. This is shown graphically in figure 4.2; a plot of gamma versus stratospheric temperature for data from this work, and estimated results from Hanson and Ravishankara, (1994). All data is summarized in tables 4.1 and 4.2. Figure 4.2 shows that reaction probabilities from this work are slightly lower than those reported by Hanson and Ravishankara.

These studies showed that there is a strong dependence of γ on HCl weight fraction; indeed, additional evidence implies that the weight fraction of HCl in the solutions is the parameter that controls the reaction probability.

4.2.1 Effect of HNO_3

Figure 4.2 shows that the incorporation of HNO_3 into the sulfuric acid solutions lowers the reaction probabilities relative to solutions without HNO_3 only a small amount, despite the presence of HNO_3 levels as high as 28.3%. A study was also done by Zhang *et al.* (1994) that compared reaction probabilities with and without HNO_3 for one solution and found no change in the reaction probability.

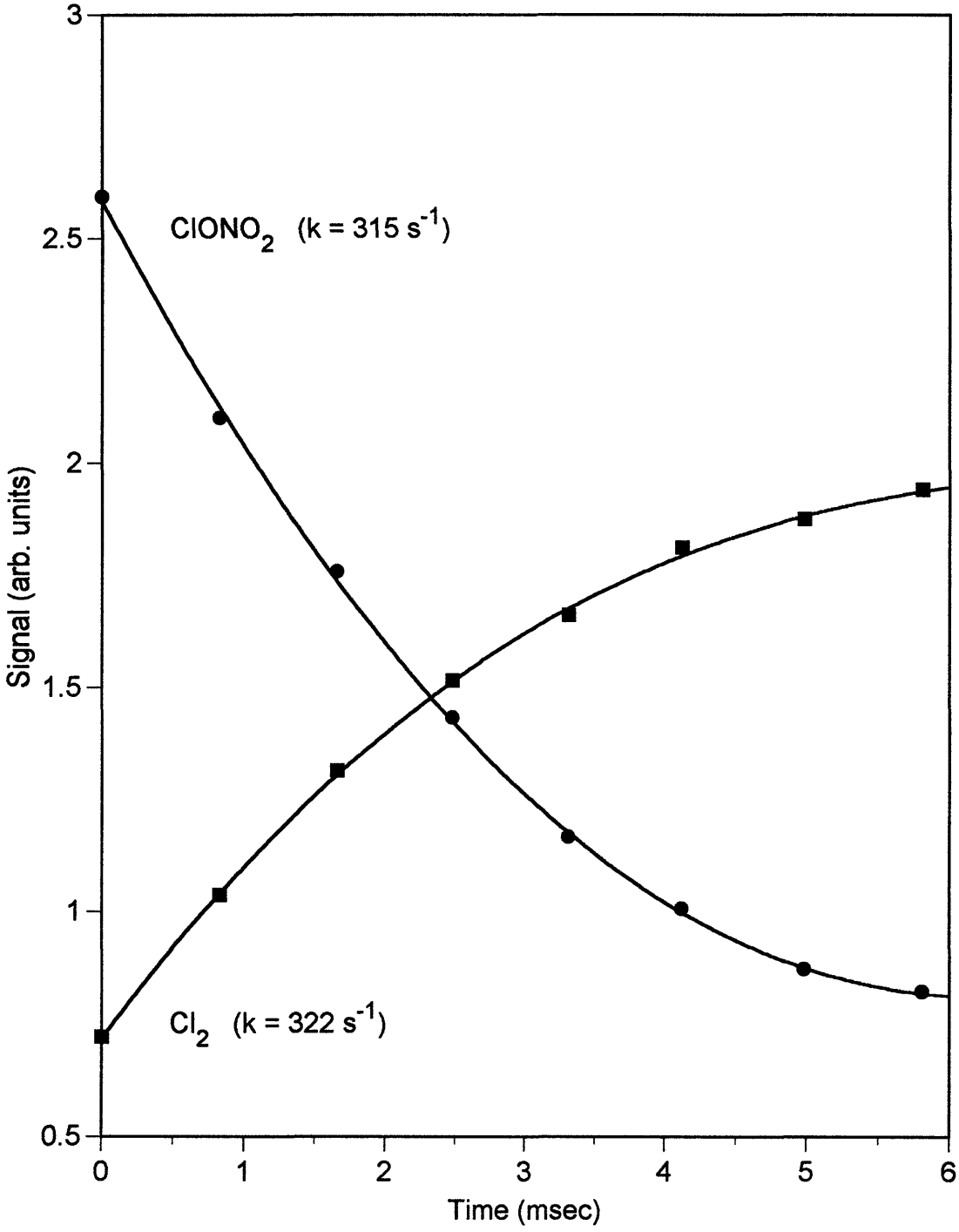

Figure 4.1 Loss and production curves for the HCl + $ClONO_2$ reaction on the 198 K (no HNO_3) solution measured at a laboratory temperature of 213 K

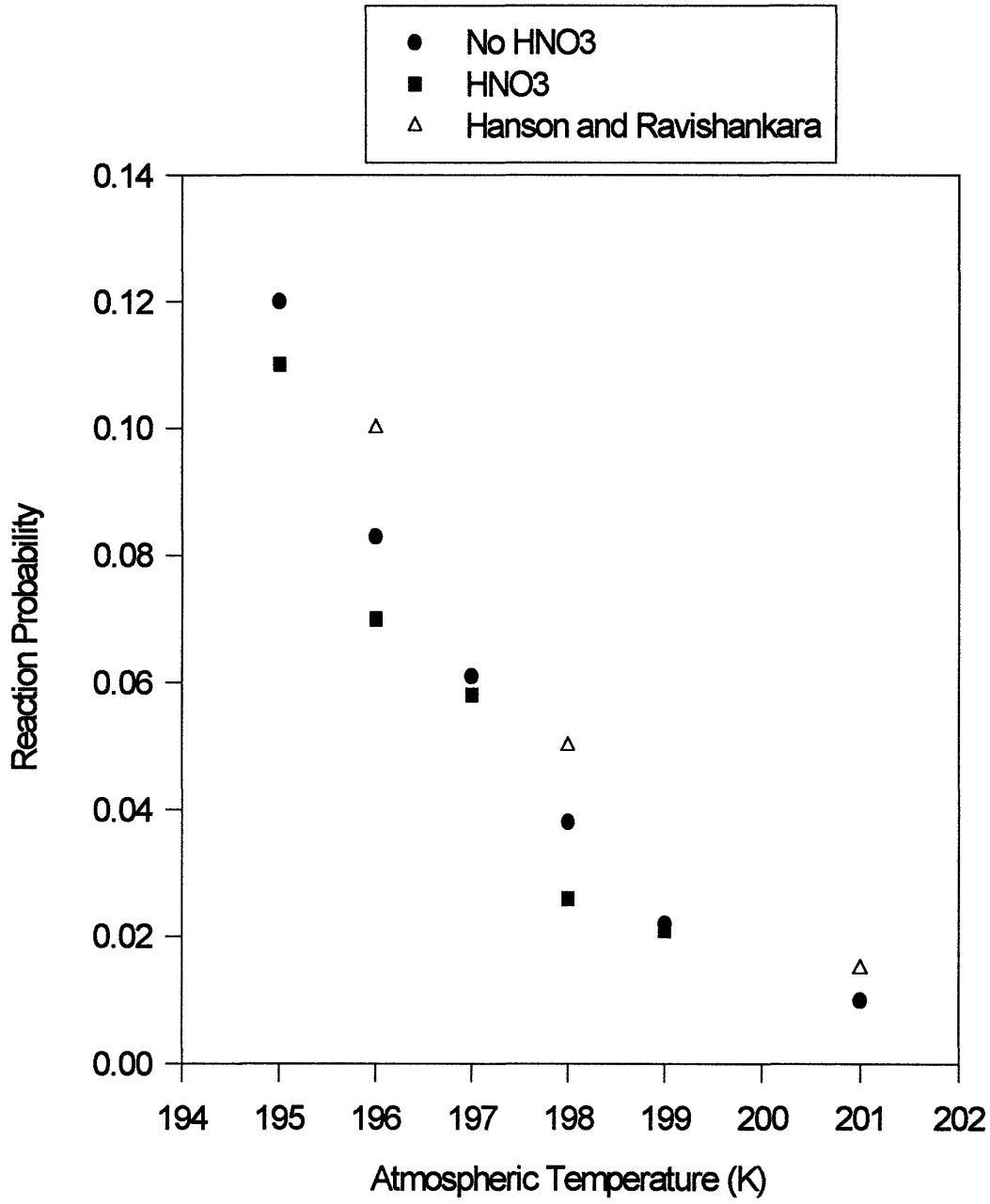

Figure 4.2 Reaction probability measurements for HCl + $ClONO_2$ as a function of atmospheric temperature assuming 5 ppmv H_2O and 2 ppbv HCl at 100 mbar. Circles represent data for solutions without HNO_3. Squares represent data with HNO_3. Open triangles are estimated data from Hanson and Ravishankara, (1994).

Temperature (K)	Weight Fraction H_2SO_4	Weight Fraction HCl	Reaction Probability
201	0.552	3.00 x 10-6	0.010
199	0.520	1.60 x 10-5	0.022
198	0.510	2.40 x 10-5	0.038
197	0.490	6.00 x 10-5	0.061
196	0.470	1.40 x 10-4	0.083
195	0.450	3.44 x 10-4	0.12
194	0.430	8.24 x 10-4	0.30

Table 4.1 Reaction probabilities for Ternary $H_2SO_4/H_2O/HCl$ system, as a function of atmospheric equilibrium temperature. Measurements were made at 203 K.

Temperature (K)	Weight Fraction H_2SO_4	Weight Fraction HNO_3	Weight Fraction HCl	Reaction Probability
199	0.503	0.022	1.38 x 10-5	0.021
198	0.480	0.035	2.70 x 10-5	0.026
197	0.440	0.061	6.18 x 10-5	0.058
196	0.362	0.126	1.76 x 10-4	0.070
195	0.202	0.283	4.88 x 10-4	0.110

Table 4.2 Reaction probabilities for the Quaternary $H_2SO_4/HNO_3/H_2O/HCl$ System as a function of stratospheric equilibrium temperature. Measurements were made at 203 K.

4.2.2 H_2SO_4 Dependence

In order to examine the dependence of γ on H_2SO_4 concentration, several solutions were prepared with H_2SO_4 compositions that varied from 40% to 60%, with a fixed HCl concentration of 2.3 x 10^{-3} M. This HCl composition corresponds to a stratospheric equilibrium temperature of 197 K. The reaction probabilities are shown in table 4.3. It is

apparent that γ doesn't change much over this range of H_2SO_4, so for typical stratospheric conditions, the H_2SO_4 concentration has a negligible effect on the reaction probability.

Weight % H_2SO_4	Reaction Probability (γ)
60	.054
55	.059
51	.061
45	.046
40	.057

Table 4.3 Reaction probabilities for changing H_2SO_4 solutions with the weight per cent HCl held constant at 2.3×10^{-3} M (the concentration corresponding to a stratospheric equilibrium temperature of 197 K, no HNO_3)

4.2.3 Temperature Dependence

The laboratory temperature was varied from 203-233K for the solution corresponding to an atmospheric equilibrium temperature of 197 K (no HNO_3). These results are shown in table 4.4. The variation in γ was on the order of experimental error. This is consistent with all other measurements.

Stratospheric Temperature	Reaction Probability
203	.056
213	.061
223	.048
233	.049

Table 4.4: Effect of changing laboratory temperatures for a fixed composition corresponding to an atmospheric equilibrium temperature of 197 K (no HNO_3)

4.2.4 HCl Dependence

There still remains a need to further paramaterize this reaction in terms of HCl concentration. Hanson and Ravishankara measured γ over a large range of HCl partial pressure. As would be expected at low P_{HCl}, the $ClONO_2$ rate is dominated by hydrolysis and is independent of P_{HCl}. For intermediate P_{HCl} values, γ was found to be proportional to $(P_{HCl})^{1/2}$; for high concentrations, γ was found to be proportional to P_{HCl}.

The data presented in this work shows a square root dependence on the weight fraction of HCl, which is consistent with the Hanson and Ravishankara data, since measurements were done in the range corresponding to their intermediate concentrations. The measurements of Zhang *et al.* (1994). were carried out at high HCl concentrations and their data indicates linear proportionality between gamma and P_{HCl}. It is worthy of further study, to understand what happens in the transition region from high to low HCl concentration. Hanson and Ravishankara have indicated that this change in HCl dependence is indicative of a change from a regime where the reaction takes place mainly in the bulk to a regime where the reaction takes place on the surface. If there is indeed a transition from bulk reaction to surface reaction, this is an important factor because it has implications about the way laboratory results should be extrapolated to the stratosphere.

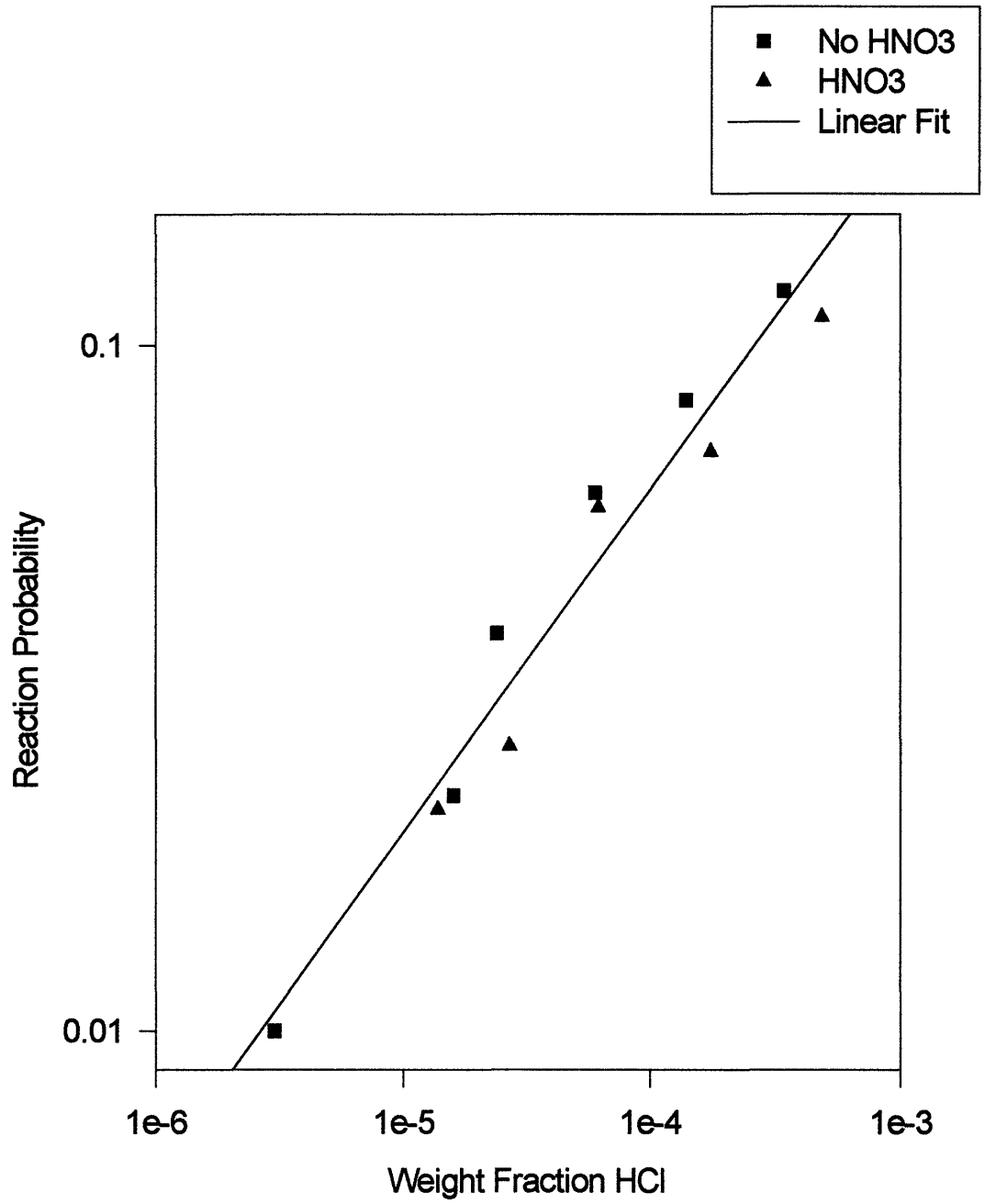

Figure 4.3 Reaction probability as a function of weight fraction HCl. Squares represent solutions without HNO_3, circles solutions with HNO_3. The line is a fit through the data; its slope is 0.545.

Chapter 5
Conclusion

5.1 Summary

The data presented here gives important information about heterogeneous reactions on sulfuric acid aerosols. The vapor pressure measurements presented here help predict stratospheric equilibrium concentrations for aerosols, but more importantly, by validating the model of Carslaw *et al.*, confirm that the concentrations of aerosols can be predicted, and used to understand heterogeneous reactions.

The measured reaction probabilities provide important insight into the kinetics of the reactions studied. Evidence implies that HCl is the controlling parameter in the HCl + $ClONO_2$ reaction. The incorporation of HNO_3 has little effect on reaction probabilities. Most importantly, the large reaction probability on aerosols with compositions

corresponding to cold stratospheric temperatures give validity to the theory that sulfate aerosols are important to ozone depletion in polar regions, and at high latitudes.

5.2 Future Research

The question of mid-latitude chlorine activation remains unanswered. The wetted-wall technique described here provides an experimental apparatus suitable for studying heterogeneous reactions on wetted-wall films. This apparatus can be used to examine the behavior of heterogeneous reactions 1.17-1.21 on both quaternary and ternary solutions.

Since heterogeneous reactions on sulfate aerosols become efficient at low stratospheric temperatures, and there are important implications for ozone depletion, it is important to fully characterize these reactions for a broad range of conditions.

As mentioned in Chapter 4, there is some ambiguity as to the functional dependence of the reaction probability on [HCl]. General trends have been noted: at low HCl concentrations, the measured γ is that of the hydrolysis reaction and is thus independent of [HCl]. At intermediate concentrations, γ is proportional to the square root of the HCl concentration, and at high concentrations, it is proportional to the HCl concentration. These dependencies need to be carefully explored for a wide range of HCl concentration with special attention paid to transition regions.

To this end, instrument modifications could provide more sensitivity and provide more information about reaction 1.17, and eventually other heterogeneous reactions:

All previous experiments have been done using an electron impact (EI) mass spectrometry detection scheme which is neither as selective or as sensitive to the species

of interest as the proposed technique, chemical ionization (CI). In the EI scheme, molecules are directly ionized with a high energy electron source (70eV). This source operates at 10^{-6} Torr, so only a small portion of the gas flow is actually ionized; the rest is pumped away before reaching the ionization region. Because of the high energy electrons that are used, much excess energy is transferred to the gaseous molecules during ionization. The excited molecules undergo unimolecular decomposition producing a great deal of fragmentation, often leaving no trace of the parent peak. This is a big problem for the reaction of interest because both $ClONO_2$ and HNO_3 fragment to form NO_2^+ at m/z=46. This makes it impossible to differentiate between $ClONO_2$ and HNO_3 for our solutions which contain HNO_3. In addition, EI is limited in sensitivity because the ionization efficiency isn't very high because there are few collisions at low pressures.

In the CI scheme, ionization occurs at the pressure of the flow tube (1 Torr) via ion molecule reactions with a reagent gas such as SF_6. When SF_6 passes through a discharge, it readily attaches an electron and forms the species SF_6^-
which reacts selectively with the species of interest, either by transferring an electron or a fluoride ion. Since the relevant CI reactions are exothermic on the order of 1-2 eV, not as much fragmentation occurs and in most cases, the parent ion is preserved. The species of interest can be uniquely detected as follows:

$$SF_6^- + Cl_2 \rightarrow Cl_2^- + SF_6 \qquad (m/z=70)$$

$$SF_6^- + ClONO_2 \rightarrow ClONO_2F^- + SF_5 \qquad (m/z=116)$$

$$SF_6^- + HNO_3 \rightarrow HNO_3F^- + SF_5 \qquad (m/z=82)$$

In addition, the CI scheme will provide more sensitivity and allow a wider range of experimental conditions to be explored. Since ionization occurs outside the vacuum chamber housing the quadrapole analyzer, at much higher pressures than in EI, the ionization efficiency is potentially higher since more collisions occur. Also, the differential pumping scheme combined with charged lenses serve to enrich the portion of the gas reaching the quadrapole analyzer with charged species, leading to better detection.

The CI detection scheme has been successfully implemented in our lab at atmospheric pressure. All the species mentioned above have been successfully detected. In other labs, CI has been implemented at the proposed pressures of 0.2 - 2 Torr. Hanson and Ravishankara (1991) can detect approximately 10^8 molecules cm^{-3}. Leu *et al.* (1995) quotes a sensitivity of 6×10^{-9} Torr for HNO_3 in a system where the ionization occurs at 0.2-0.5 Torr. The best sensitivity in the EI system previously used is 1×10^{-7} Torr for HCl.

References

1. J.P.P Abbatt and M.J. Molina, Heterogeneous interaction of $ClONO_2$ and HCl on NAT at 202 K, *J.Phys. Chem.*, **96**, 7674, 1992a.

2. Abbatt and M.J. Molina, The heterogeneous reaction of HOCl + HCl $\rightarrow$ Cl_2 + H_2O on ice and nitric acid trihydrate: Reaction probabilities and stratospheric implications, *Geophys. Res. Lett.* **19**, 461, 1992b.

3. Anderson, J.G., D.W. Toohey, and W.H. Brune, Free radicals within the Antarctic vortex: The role of CFCs in Antarctic O_3 loss, *Science*, **251**, 39, 1991.

4. Arnold, F., Th. Buhrke, and S. Qiu, Evidence for stratospheric ozone-depleting heterogeneous chemistry on volcanic aerosols from El Chichon, *Nature*, **348**, 49, 1990.

5. Bates, D.R., and M. Nicolet, *J. Geophys. Res.* **55**, 30, 1950.

6. Beyer, K.D., S.W. Seago, H.Y. Chang, and M.J. Molina, Composition and freezing of aqueous H_2SO4/HNO_3 solutions under polar stratospheric conditions, *Geophys. Res. Lett.* **21**, 871, 1994.

7. Brown, R.L., Tubular flow reactors with first-order kinetics, *J. Res. Natl. Bur. Stand.* **83**, 1, 1978.

8. Carslaw, K.S., B.P. Luo, S.L. Clegg, T. Peter, P. Brimblecombe and P.J. Crutzen, Stratospheric aerosol growth and HNO_3 gas phase depletion from coupled HNO_3 and water uptake by liquid particles, *Geophys. Res. Lett.*, **21**, 2479, 1994.

9. Carslaw, K.S., S.L. Clegg, and P. Brimblecombe, A thermodynamic model of the system $HCl-HNO_3-H_2SO_4-H_2O$, including solubilities of HBr, from <200 to 328 K, *J. Phys. Chem.* **99**, 11557, 1995.

10. Chapman, S., A theory of upper-atmosphere ozone. *Mem. Roy. Meteorol. Soc.*, **3**, 103, 1930.

11. Danckwerts, P.V., Gas-Liquid Reactions, McGraw Hill Book Company, 1970.

12. Drdla, K., A. Tabazadeh, R.P. Turco, M.Z. Jacobson, J.E. Dye. C. Twohy, and D. Baumgardner, Analysis of the physical state of one Arctic polar stratospheric cloud, based on observations, *Geophys. Res. Lett.*, **21**, 2475, 1994.

13. Elrod, M.J., R.E. Koch, J.E. Kim, and M.J. Molina, The role of nitric acid in the $ClONO_2$ + HCl reaction on sulfuric acid surfaces, *Faraday Discuss.*, 1995, **100**, 269.

14. Farman, J.C., B.G. Gardiner and J.D. Shanklin, Large losses of total ozone in Antarctica reveal seasonal ClO_x/NO_x interaction, *Nature*, **315**, 207, 1985.

15. Fritz, J.J. and C.R. Fuget, *Chem. Eng. Data Ser.* **1,** 19, 1956.

16. Golden, D.M., J.A. Manion, C.M. Reihs, and M.A. Tolbert, Heterogeneous chemistry on global stratospheric particulate: Reaction of $ClONO_2$ and N_2O_5 on sulfuric acid surfaces, in *The Chemistry of the Atmosphere: Its Impact on Global Change,* ed. J.G. Calvert, Blackwell Scientific, Boston, Mass. 1994, p. 39.

17. Hanson, D.R. and A.R. Ravishankara, The reaction probabilities of $ClONO_2$ and N_2O_5 on 40 to 75 % sulfuric acid solutions, *J. Geophys. Res.*, **96,** 17307, 1991.

18. Hanson, D.R., and A.R. Ravishankara, Uptake of HCl and HOCl onto sulfuric acid: Solubilities, diffusivities, and reaction, *J. Phys. Chem.*, **97**, 12309, 1993.

19. Hanson, D.R., and A.R. Ravishankara, Reactive uptake of $ClONO_2$ onto sulfuric acid due to reaction with HCl and H_2O, *J. Phys. Chem.*, **98**, 5728, 1994.

20. Hanson, D.R., A.R. Ravishankara and S. Solomon, Heterogeneous reactions in sulfuric acid aerosols: A framework for model calculations, *J. Geophys. Res.*, **99**, 3615, 1994.

21. Hofmann, D.J., and S. Solomon, Ozone destruction through heterogeneous chemistry following the eruption of El Chicon, *J. Geophys. Res.*, **94**, 5029, 1989.

22. Howard, C.J., Kinetics measurements using flow tubes, *J. Phys. Chem.* **83**, 3, 1979.

23. Kawa, S.R., D.W. Fahey, K.K. Kelly, J.E. Dye, D. Baumgardner, B.W. Gandrud, M. Loewenstein, G.V. Ferry and K.R. Chan, The Arctic polar stratospheric cloud aerosol: Aircraft measurements of reactive nitrogen, total water and particles, *Geophys. Res.*, **97**, 7925. 1992.

24. Leu, M-T, R.S. Timonen, L.F. Keyser and Y.L. Yung, *J. Phys. Chem.* **99,** 13203, 1995.

25. Lovelock, J.E., R.J. Maggs and R.J. Wade, Halogenated hydrocarbons in and over the Atlantic. *Nature*, **241**, 194, 1973.

26. McCormick, H.M. Steele, P. Hamill, W.P. Chu and T.J. Swissler, Polar stratospheric cloud sightings by SAM II, *J. Atmos. Sci.* **39**, 1387, 1982.

27. McElroy, R.J. Salawitch, S.C. Wofsy, and J.A. Logan, Reduction of Antarctic ozone due to synergistic interactions of chlorine and bromine, *Nature*, **321**, 759, 1986.

28. Molina, L.T. and Molina, M.J., Production of Cl_2O_2 from the self reaction of the ClO radical. *J. Phys. Chem.*, **91**, 433, 1987.

29. Molina, L.T., M.J. Molina, R.A. Stachnic, and R.D. Tom, An upper limit for the rate of the HCl + $ClONO_2$ Reaction, *J. Phys. Chem.* **89**, 3779, 1985.

30. Molina, M. J., The Probable Role of Stratospheric Ice Clouds: Heterogeneous Chemistry of the Ozone Hole, in *The Chemistry of the Atmosphere: Its Impact on Global Change,* ed. J.G. Calvert, Blackwell Scientific, Boston, Mass. 1994, p. 27.

31. Molina, M. J. and F.S. Rowland, Stratospheric sink for chlorofluoromethanes: chlorine atom-catalysed destruction of ozone. *Nature,* **249**, 810, 1974.

32. Molina, M.J., T.L. Tso, L.T. Molina, and F.C.Y. Wang, Antarctic stratospheric chemistry of chlorine nitrate, hydrochloric acid, and ice: Release of active chlorine, *Science*, **261**, 1418, 1993.

33. Molina, M.J., R. Zhang, P.J. Wooldridge, J.R. McMahon, J.E. Kim, H.Y. Chang, and K.D. Beyer, Physical chemistry of the $H_2SO_4/HNO_3/H_2O$ system: Implications for polar stratospheric clouds, *Science*, **261**, 1418, 1993.

34. Mozurkewich, M., and J.G. Calvert, Reaction probability of N_2O_5 on aqueous aerosols, *J. Geophys. Res.* **93**, 15889, 1988.

35. Pool, R., The Elusive Replacements for CFCs, *Science*, **242**, 666, 1988.

36. Reihs, C.M., D.M. Golden and M.A. Tolbert, Nitric acid uptake by sulfuric acid solutions under stratospheric conditions: Determination of Henry's law solubility, *J. Geophys. Res.*, **95**, 16545, 1990.

37. Rodriguez, J.M., M.K.W. Ko and N.D. Sze, Role of heterogeneous conversion of N_2O_5 on sulfate aerosols in global ozone loss, *Nature*, **352**, 134, 1991.

38. Rosen, J.M., The boiling point of stratospheric aerosols, *J. Appl. Meteor.*, **10**, 1044, 1971.

39. Schoeberl, M.R. and D.L Hartman, The dynamics of the stratospheric polar vortex and its relations to springtime ozone depletion, *Science*, **251**, 46, 1991.

40. Solomon, S., The Mystery of the Antarctic ozone "hole," *Rev. Geophys.* **26,** 131, 1988.

41. Solomon, S., R.R. Garcia, F.S. Rowland, and D.J. Wuebbles, On the depletion of Antarctic ozone, *Nature*, **321**, 755, 1986.

42. Stanford, J.L., and J.S. Davis, A century of stratospheric cloud reports: 1870-1972. *Bull. Amer. Meteor. Soc.*, **55**, 213, 1974.

43. Steele, H.M., P. Hamill, M.P. McCormick, T.J. Swissler, The formation of polar stratospheric clouds. *J. Atmos. Sci.*, **40**, 2055, 1983.

44. Tabazadeh, A., R.P Turco, and M.Z. Jacobson, A model for studying the composition and chemical effects of stratospheric aerosols, *J. Geophys. Res*, **99**, 12897, 1994.

45. Tolbert, M.A., M.J. Rossi, and D.M. Golden, Heterogeneous interactions of chlorine nitrate, hydrogen chloride, and nitric acid with sulfuric acid surfaces at stratospheric temperatures, *Geophys. Res. Lett.*, **15**, 847, 1988.

46. Toon, O., E. Browill, B. Gary, L.Lait, J. Livingston, P. Newman, R. Pueschel, P. Russell, M. Schoeberl, G. Toon, W. Traub, F.P.J. Valero, H. Selkirk, and J. Jordan, Heterogeneous reaction probabilities, solubilities, and physical state of cold volcanic aerosols, *Science*, **261**, 1136, 1993.

47. Toon, O.B., and M.A. Tolbert, Spectroscopic evidence against nitric acid trihydrate in polar stratospheric clouds, *Nature*, **375**, 218, 1995.

48. Utter, R.G., J.B. Burkholder, C.J. Howard, and A.R. Ravishankara, Measurement of the mass accomodation coefficient of ozone on aqueous surfaces, *J. Phys. Chem.*, **96**, 4973, 1992.

49. Van Doren, J.M., L.R. Watson, P. Davidovits, D.R. Worsnop, M.S. Zahniser, and C.E. Kolb, Uptake of N_2O_5 and HNO_3 by aqueous sulfuric acid droplets, *J. Phys Chem.*, **95**, 1684, 1991.

50. Watson, L.R., J.M. Van Doren, P. Davidovits, D.R. Worsnop, M.S. Zahniser and C.E. Kolb, Uptake of HCl molecules by aqueous sulfuric acid droplets as a function of acid concentration. *J. Geophys. Res.*, **95**, 5631, 1990.

51. Wayne, R.P. *Chemistry of Atmospheres.* Oxford University Press, 1991.

52. Williams, L.R. and D.M. Golden. Solubility of HCl in sulfuric acid at stratospheric temperatures. *Geophys. Res. Lett.* **20**, 2227, 1993.

53. Zhang, R. P.J. Wooldridge, and M.J. Molina, Vapor pressure measurements for the $H_2SO_4/HNO_3/H_2O$ and $H_2SO_4/HCl/H_2O$ systems: Incorporation of stratospheric acids into background aerosols, *J. Phys. Chem.*, **97**, 8541, 1993.

54. Zhang, R., M.-T. Leu, and L.F. Keyser, Heterogeneous reactions of $ClONO_2$, HCl and HOCl on liquid sulfuric acid surfaces, *J. Phys. Chem.*, **98**, 13563, 1994.